UCRL-16913

University of California

Ernest O. Lawrence Radiation Laboratory

THE $C^{12}(p, 2p)B^{11}$ REACTION AT 50 MeV

Berkeley, California

DISCLAIMER

Submitted to Physical Review

UCRL-16913

UNIVERSITY OF CALIFORNIA

Lawrence Radiation Laboratory
Berkeley, California

AEC Contract No. W-7405-eng-48

THE $C^{12}(p,2p)B^{11}$ REACTION AT 50 MeV

H. G. Pugh, D. L. Hendrie, Marc Chabre, E. Boschitz and I. E. McCarthy

August 1966

THE $C^{12}(p,2p)B^{11}$ REACTION AT 50 MeV*

H. G. Pugh†, D. L. Hendrie, Marc Chabre** and E. Boschitz‡

Lawrence Radiation Laboratory
University of California
Berkeley, California

and

I. E. McCarthy

University of Oregon
Eugene, Oregon

ABSTRACT

The $C^{12}(p,2p)B^{11}$ reaction has been studied at a bombarding energy of 50.0±0.2 MeV with an energy resolution of 300 keV. Transitions were observed to the ground state and to the 2.14, 4.46, 5.04 and 6.76 MeV excited states of B^{11}. Angular correlation measurements have been made in various coplanar geometrical arrangements. In the symmetric geometry, where the protons are detected at equal angles on either side of the incident beam direction, the angular correlation was measured from 15° to 115°. In an asymmetric geometry in which one detector was fixed at 30°, measurements were made as the other detector was moved between 15° and 100° on the other side of the beam direction. Both of the angular correlations are characterized by a general rise in the forward direction, modulated by a diffraction-like structure, when only those events are selected in which the energies of the selected protons are equal. The results of a distorted wave analysis are presented and discussed. The formation of the 4.46 MeV (5/2-) and 6.76 MeV (7/2-) states is discussed in terms of the ejection of a proton from the 1f shell in C^{12} and more attractively, in terms of a two-stage process involving both the ejection of a 1p-state proton and a core excitation

I. INTRODUCTION

The study of (p,2p) reactions has become, over the last several years, an established method for studying nuclear structure.[1] Most experiments have been in the energy range above 150 MeV and most theoretical analyses have been in terms of the impulse approximation with semiclassical corrections for absorption of the incoming and outgoing protons by the residual nucleus. A review article by Jacob and Maris[2] summarizes the present experimental and theoretical situation from the above viewpoint.

We have been led to study the (p,2p) reaction at 50 MeV by both experimental and theoretical considerations. The experimental considerations are those of energy resolution, duty factor and beam intensity. In the high-energy experiments the energy resolution has not been adequate to resolve individual states of the residual nucleus. Because of this it has not been worthwhile to consider the data in terms of nuclear models more refined than the j-j coupled spherical shell model. Several authors[3] have used more sophisticated models to predict which states should be observed with improved energy resolution, but no direct verification has been given. Using the new sector-focused cyclotrons and solid-state particle detectors it is now easy to obtain energy resolution of a few hundred kilovolts, about ten times better than previously attained.[4] Moreover, the improved duty factor and higher beam intensity of the new cyclotrons makes it possible to observe the reaction over a wider angular range than has previously been feasible, and to make a more detailed examination of the available phase space. On the other hand, the reaction at 50 MeV is much more limited by kinematic factors than at higher energies: it is not energetically possible

to observe the highly excited states of the residual nucleus which correspond to the removal of deeply bound protons from the target, nor is the range of phase space available for a given transition as large.

Theoretical considerations which make 50 MeV an interesting energy for studying (p,2p) reactions are several. Primarily the reasons which lead to the choice of much higher bombarding energies for spectroscopic studies[5] are exactly those which cause increased interest in the reaction mechanism at lower energies. Lim and McCarthy[6] have shown that within the accuracy of experiments so far performed it is not possible at 150 MeV to distinguish between the impulse approximation and the distorted-wave t-matrix approximation. Simple treatments of wave distortion have been shown to be sufficient at the higher bombarding energies. It is in the low energy region that off-energy-shell effects will be most important and that distortion effects may produce significant changes in the reaction mechanism. One possible complication that may arise at these energies is that the reaction will cease to be a pure direct single-stage reaction and compound nucleus effects will contribute. Detenbeck[7] has found, for example, that the $N^{14}(p,2p)C^{13}$ reaction proceeds in two stages at 19 MeV. The choice of C^{12} for the target was made for several reasons. This target has been extensively studied at higher energies. The binding-energy of the protons is large so that the scattering is far from the energy shell. Finally, its structure has been well investigated, having a large component of a closed $p_{3/2}$ proton shell in the j-j coupling model.

II. THEORY

In a (p,2p) experiment the momenta of both protons in the final state are measured so that the momentum transferred to the residual nucleus (core) is completely specified. The three-body nature of the final state allows a wide choice of regions of phase space in which momentum transfer distributions can be measured. The theoretical understanding of the reaction is simplified if it can be considered as a direct interaction. For this reason it is advantageous to observe the final states in regions of phase space where the relative energies of the three particles are such that the proton-core and proton-proton scattering amplitudes are all smoothly varying functions of energy. The two-body scattering amplitudes may then be described by a potential model, where the potential that describes the proton-core interaction is complex. This is the simplest approximation that allows for the fact that more than one channel is excited in the reaction.

The experiment is understood as a quasi-three-body reaction in which a bound proton is removed from the core. The simplest such reaction is one in which the core is not excited. If the core is excited the theory must include a description of the excitation mechanism as well as a description of the knock-out process. The first step in a detailed theoretical description is to understand the knock-out process itself without the complication of core excitation. For this purpose the bound state wave function is chosen to be a 1p wave function in a massive central square well of 3.5 Fm radius.[6] The depth of the well is selected to give a correct binding energy of the proton of 16 MeV. This choice yields good fits to the $C^{12}(p,2p)B^{11}$ data at 155 MeV and is consistent with electron scattering measurements.

At incident energies above about 150 MeV the distorted wave impulse approximation has been shown by many authors[1,8] to be sufficient to fit the data. Lim and McCarthy[6] showed that for $C^{12}(p,2p)B^{11}$ at 155 MeV the distorted wave impulse approximation is as good as the distorted wave t-matrix approximation for the same proton-proton and proton-core interactions. Jackson and Berggren[9] showed that at 180 MeV the eikonal approximation is sufficient for the distorted waves.

The difference between the distorted wave impulse and t-matrix approximations is that the impulse approximation uses only information about the two body amplitudes on the energy shell; this is the information which can be obtained from scattering experiments. The distorted wave t-matrix approximation uses a finite range pseudopotential description of the (p,p) interaction which is a model for the (p,p) t-matrix off the energy shell. It uses proton-core wave functions, computed from two-body scattering data, that are on the energy shell, but the distortion results in off-shell (p,p) amplitudes playing a part in the calculation. The p-p pseudopotential used in this work is parameterized in the following way:[6]

$$v(r) = A_{10}v_0\left[e^{-\mu_1 r}/\mu_1 r + a_2\, e^{-\mu_2 r}/\mu_2 r + a_3\, e^{-\mu_3 r}/\mu_3 r\right] , \qquad (1)$$

where $A_{10}v_0 = -83$ MeV, $\mu_1 = 0.73$ Fm^{-1}, $\mu_2 = 1.5$ Fm^{-1}, $\mu_3 = 3.0$ Fm^{-1}, $a_2 = -5$ and $a_3 = 20$.

There are two parameters, A_{10} and A_{11}, to the pseudopotential,[13] one describing scattering in the singlet even state, and one in the triplet-odd state. The former is determined by fitting (1) to the differential cross-section for p-p scattering as

a function of energy. The pseudopotential for the triplet state, taken as a constant (A_{11}/A_{10}) times (1), is not determined by scattering and (A_{11}/A_{10}) is treated as a parameter to be determined from the fit to the $C^{12}(p,2p)B^{11}$ data.

Both approximations have conceptual difficulties. For the impulse approximation the momentum transfer and incident energy in the free (p,p) experiment which correspond to a particular momentum transfer in the (p,2p) experiment are not uniquely defined by the theory. In early calculations semi-classical assumptions were made for the "internal (p,p) collision". The difficulty of the t-matrix approximation is that the off-shell (p,p) amplitudes are not known from a scattering experiment. The three-body experiment may be regarded as determining them. In this the (p,2p) experiment is complementary to two free nucleon experiments. However we must have a good model for a three-body problem if the determination is to be meaningful.

The distorted wave t-matrix approximation matrix element is[10]

$$T = \int d^3r_1 \int d^3r_2 \chi^{(-)*}(\underset{\sim}{k}_L, \underset{\sim}{r}_1)\chi^{(-)*}(\underset{\sim}{k}_R, \underset{\sim}{r}_2)v(|\underset{\sim}{r}_1 - \underset{\sim}{r}_2|)\chi^{(+)}(\underset{\sim}{k}_0, \underset{\sim}{r}_1)\psi_L^M(\underset{\sim}{r}_2) \qquad (2)$$

where $\chi^{(+)}(\underset{\sim}{k}_0, \underset{\sim}{r}_1)$ and $\chi^{(-)}(\underset{\sim}{k}, \underset{\sim}{r})$ are the incoming and outgoing distorted wave, respectively, $v(|\underset{\sim}{r}_1 - \underset{\sim}{r}_2|)$ is the pseudopotential of (1) and $\psi_L^M(\underset{\sim}{r}_2)$ is the bound state wave function of the struck proton.

If the Fourier transform of the optical model wave function $\chi^{(\pm)}(\underset{\sim}{k}_i, \underset{\sim}{r})$ is denoted by $\phi^{(\pm)}(\underset{\sim}{k}_i, \underset{\sim}{k})$ and that of $\psi_L^M(\underset{\sim}{r})$ by $\phi_L^M(\underset{\sim}{k})$, Eq. (2) can be re-written as

$$T = \int d^3k \int d^3k' \int d^3k'' \int d^3k''' \; \phi^{(-)*}(\underset{\sim}{k}_L, \underset{\sim}{k}) \phi^{(-)*}(\underset{\sim}{k}_R, \underset{\sim}{k}') \phi^{(+)}(\underset{\sim}{k}_0, \underset{\sim}{k}'') \phi_L^M(\underset{\sim}{k}''')$$

$$\times v(\underset{\sim}{k}, \underset{\sim}{k}', \underset{\sim}{k}'', \underset{\sim}{k}''') \quad . \tag{3}$$

Notice that the Fourier coefficients would be delta functions for the case of free (p,p) scattering.

The (p,p) scattering amplitude

$$v(\underset{\sim}{k}, \underset{\sim}{k}', \underset{\sim}{k}'', \underset{\sim}{k}''') = \int d^3r_1 \int d^3r_2 e^{-i\underset{\sim}{k}\cdot\underset{\sim}{r}_1 - i\underset{\sim}{k}'\cdot\underset{\sim}{r}_2} v(|\underset{\sim}{r}_1 - \underset{\sim}{r}_2|) \; e^{i\underset{\sim}{k}''\cdot\underset{\sim}{r}_1 + i\underset{\sim}{k}'''\cdot\underset{\sim}{r}_2} \tag{4}$$

is present for all possible values of the arguments, including those which do not conserve momentum. If $v(|\underset{\sim}{r}_1 - \underset{\sim}{r}_2|)$ is a pseudopotential the expression (4) is a model for the actual (p,p) amplitude when momentum is conserved.

Because focus effects in the final state proton-core wave functions cause large distortions at 50 MeV incident energy, this energy is very useful for examining the question of whether the distorted wave t-matrix approximation itself, on which all present understanding of the (p,2p) reaction is based, is a good three-body model. It certainly contains three-body effects at 50 MeV, in the sense that off-shell (p,p) amplitudes are important. The question is whether they are the right three-body effects.

III. EXPERIMENTAL ARRANGEMENT AND PROCEDURE

The Berkeley 88-inch Cyclotron was used to direct a beam of 50.0±0.2 MeV protons through the center of a 17-inch scattering chamber. For this experiment the beam, after being energy analysed to an energy spread of less than 100 keV,

was focused without further collimation to a 1 mm × 1 mm spot on the target with an angular divergence less than 0.5 deg. Beam intensities ranged from 1 to 50 nA. The self supporting target, 2.3±0.1 mg/cm^2 thick, was made by heating filter paper first in air and then in vacuo. Beam currents were read in a Faraday cup and integrated electronically.

The outgoing proton pairs were detected in two independently movable coplanar solid-state detector telescopes mounted in the equatorial plane of the scattering chamber. Each telescope consisted of a 0.5 mm lithium-drifted silicon ΔE, and a 3 mm lithium-drifted silicon E detector. Protons of energy less than 9 MeV would not penetrate the ΔE counter, and protons of energy greater than 25 MeV would pass completely through both counters, providing the energy limits over which the outgoing protons could be usefully detected. Since the Q-value for the $C^{12}(p,2p)B^{11}$ reaction is -16.0 MeV, a maximum of 34 MeV is available to share between the outgoing protons. By imposing the requirement that each proton shall pass through the ΔE detector and thus have at least 9 MeV, we ensure that the energy of each proton shall also be less than 25 MeV and fall within the range of the E detector.

The counter apertures were defined by tantalum collimators 10.16 cm from the target, each of which subtended 6.9×10^{-3} steradians. For most of the symmetric counter work, a 0.955 cm diameter circular collimator was used which gave an angular acceptance of 5.40°. The rest of the work employed a square collimator of side 0.838 cm, yielding a horizontal acceptance angle of 4.7°.

A schematic block diagram of the electronics is shown in Fig. 1. Essentially all the operations were performed within the Goulding-Landis system. The fourfold fast coincidence was sufficient to resolve events originating in different r.f. beam pulses from the cyclotron but not to separate events originating in the same beam pulse. The beam structure consisted of equal intensity pulses of less than 10 nanoseconds width and spaced 65 nanoseconds apart. The single-channel pulse height analysers enabled us to remove elastic scattering events before the fast coincidence circuits. The linear gates were opened only for events in which a fourfold coincidence had been recorded. Further selection was made by two Goulding-Landis[11] particle identifiers, which ensured that each recorded event consisted of a proton detected in both counter telescopes. The adding and subtracting circuits enabled us to obtain two-dimensional displays in a form appropriate for the reaction kinematics.

An important feature of the electronics was the use of a four-fold gated pulser of good linearity and accurate timing. Pulses were fed into each preamplifier throughout the experiment and recorded with the data. By this means the amplifier gains could be adjusted and monitored. By observing the loss of pulser counts between the input and output of the whole electronic system, counting losses due to dead times and pile-up could be measured. All results have been corrected for such losses which, in general, did not exceed 5%. No separate measurements of chance coincidences were made. All the events of interest fell in sharp kinematic lines with chance coincidences forming a smooth background, which could easily be subtracted. This procedure was found to be reliable in tests made as a function of beam intensity.

The data were taken in two 80 hour runs, separated by a period of six months. Measurements repeated within each run and in the two runs separately were found to be consistent. The results displayed in the next section are shown with relative statistical errors. The absolute uncertainties are probably less than 10%.

IV. RESULTS

Figure 2 shows a sample summed energy spectrum $E_1 + E_2$ obtained with both detectors at $\theta = 35°$, averaged over the range $|E_1 - E_2| < 5$ MeV. Energy resolution of better than 300 keV permits us to separate and identify the first four states of B^{11}. These states have all previously been observed; the identification of the states observed in the present experiment is made by comparison of peak positions with pulser calibrations at various angles. The fifth state observed is indicated by our energy calibration to be the 6.76 MeV state. However, the energy resolution is not sufficient to rule out an appreciable contribution from the known state at 6.81 MeV. Nevertheless, by comparison of our spectra and angular distributions with thos of the $C^{12}(p,d)C^{11}$, $C^{12}(d,t)C^{11}$ and $C^{12}(d,He^3)B^{11}$ reactions which we have studied at the same energy, we are convinced that any contribution from the 6.81 MeV state is negligible.

A detailed discussion of the excited states will be given in section V. The remaining parts of this section are concerned with angular correlations for the ground- state transition.

A. Symmetric Counter Geometry

In this geometry the counter telescopes were moved so that they made equal angles θ on either side of the beam direction. This geometry has the feature that when $E_1 = E_2$ the recoil nucleus always moves along the beam direction. At $\theta = 32°$ the recoil nucleus has no kinetic energy for transitions to the ground state. This arrangement is that most commonly used at higher energies. Figure 3 shows the differential cross-section $d\sigma/d\Omega_1\, d\Omega_2\, d(E_1 - E_2)$ for the ground state transition, averaged over the region in which $|E_1 - E_2| < 5$ MeV. By contrast with the corresponding results at high energies we see here a rapid rise at small angles and oscillatory behavior at larger angles which is reminiscent of diffraction structure.

Figure 4 shows the (E1 - E2) spectra taken at various angles. We have studied these spectra to test for sharp structure. Such structure could appear if the reaction proceeded through long-lived proton unstable excited states of C^{12} in the excitation region between 25 and 40 MeV. Essentially no indications of structure are present. The spectra must, as a consequence of the geometry, be symmetric about E1 = E2.

If the plane-wave impulse approximation were correct the E1 - E2 spectra of Fig. 4 and the differential cross-sections of Fig. 3 would show a common dependence on the magnitude of the momentum transfer to the recoil nucleus B^{11}. In general we do not observe such a common dependence, except near zero momentum transfer to the residual nucleus, where some dependence of the cross section on momentum transfer is apparent.

We have estimated the cross section for exactly equal energy sharing, E1 = E2, by drawing smooth curves through the E1 - E2 spectra. The results are shown as a dotted line in Fig. 3.

Since the distorted wave t-matrix approximation analysis is most sensitive to the optical parameters of outgoing protons, 17-MeV protons were elastically scattered from B^{11} to obtain these parameters. The data and best fit found by search in four parameters are shown by the circles and solid line, respectively, in Fig. 5. The well used was a Woods-Saxon well with volume absorption and no spin-orbit term.

$$V(r) = -(V_o + iW)\,[1 + \exp\,(r-r_o/a)]^{-1} \qquad (5)$$

The parameters are given in column 2 of Table I, along with those used for the incoming protons as determined from the data of Craig, et al.,[12] in column 1.

Table I

	1	2	3
E(MeV)	46	17	17
target	C^{12}	B^{11}	B^{11}
V_o(MeV)	38	50	70
W(MeV)	11	8	5
r_o(fm)	1.2	1.3	1.2
a(fm)	0.5	0.5	0.5

The distorted-wave t-matrix approximation curve with the final state parameters determined by fitting elastic scattering gives an extremely poor fit to the (p,2p) data[6]; the major discrepancy is that the small angle parts of the curve are moved about ten degrees to the left in the theory.

The calculation that gave the solid line in Fig. 3 used the final state optical model parameters given in column 3 of Table I. Even if one increases r_o to 1.3 Fm and readjusts V_o to compensate for the well known $V_o r_o^2$ ambiguity, the value of V_o is still about 10 MeV larger than the value which fits elastic scattering. The parameters of column 3 yield a much worse fit to the elastic scattering as shown by the dashed line in Fig. 5.

The maximum at 100° in Fig. 3 is absent if only the singlet-even part of the (p,p) interaction is used in the theory. A triplet-odd contribution equal to about 1/3 of the singlet-even part enables this maximum to be fitted in magnitude and position. This is about the upper limit of a possible contribution determined from shell model calculations.[13]

Of the four peaks in the coplanar experiment only two can be understood as analogous to diffraction structure. These are the initial forward rise, which is enhanced by the effect of the larger (p,p) scattering amplitude at forward angles, and the 65° peak. They correspond to the first peak in the spherical Bessel function for positive and negative momentum transfer. The 40° peak is understood as a distortion effect corresponding to the filling in of the minimum observed near zero momentum transfer in (p,2p) experiments at higher energy. It is analogous to the maxima at small angles observed in (p,p') inelastic scattering for 2+ excitation where the plane wave theory predicts a minimum.

On the basis of this analysis we draw the conclusion that the three-body effects in the distorted wave t-matrix appriximation are not the right ones. These effects are introduced by the proton-core potentials causing distortion which makes the Fourier coefficients of Eq.(3) very different from δ-functions. This in turn causes large contributions from off-shell (p,p) amplitudes (Eq. (4)). In order to introduce more correct 3-body effects the feature of the calculation that introduces them, namely the proton-core potential, must be changed. There is a definite discrepancy between optical model wave functions which fit proton-core scattering in the absence of the third body and the ones which introduce the correct three body effects in the (p,2p) reaction.

B. One Fixed Counter Geometry

In order to test whether the conclusions drawn from the analysis of results of the symmetric work are generally correct and are not just a property of the rather special region of phase space observed in the coplanar symmetric experiment, further work was done in which one counter telescope, θ_1, was held fixed at 30°. The differential cross section, $d\sigma/d\Omega_1 d\Omega_2 d(E_1-E_2)$ is shown in Fig. 6, again averaged over the region $|E_1-E_2| < 5$ MeV. Again we note a sharp rise in the cross section at forward angles. The diffraction type structure is also present, but with a periodicity of about one half that seen for the symmetric work. This is not unexpected since only one counter is being moved so that the separation angle between the counters, $\theta_1 + \theta_2$, is increasing at on half the rate of the symmetric work.

If the deeper potential felt by the outgoing protons in the (p,2p) experiment than elastically scattered protons is independent of the geometry, then the best fit to the asymmetric data will be obtained with set 3 of final state potential parameters in Table I. These are the parameters which best fitted the symmetric experiment.

The theoretical curve obtained from these parameters is shown as the solid curve in Fig. 6. Many calculations with smaller values of the final state potential were performed. In these, the other parameters of the theory were varied to see if they would have the same effect as increasing V_o. They did not, and set 3 in fact provided the best fit. Any smaller value of V_o moved the curve further to the left, irrespective of the values of other parameters.

C. Other Geometries

Two other arrangements were devised to provide some insight into the features of the reaction, independent of the analysis described above.

We first tried to look at the process as a (p,He^2) pickup reaction. To do this we fixed the relative energy of the outgoing proton pair by maintaining the angle between the detectors, $\Delta\theta$, at 20° and selecting only those events in which the two protons have equal energies. The mean angle of the two counters, θ_o, was then varied from 25° to 55°. This arrangement held the relative momentum of the two outgoing protons constant at about 60 MeV/c, and varied the momentum transfer to the residual nucleus, simulating a pick-up reaction leading to a final unbound di-proton of about

1-MeV internal energy. The angular distribution obtained this way is shown in Fig. 7(a) where again $|E_1-E_2| < 5$ MeV. The cross section drops smoothly with increasing mean angle, and thus with increasing momentum transfer to the recoiling B^{11} nucleus, which varied from about 150 to 300 MeV/c. These rather rough results are qualitatively as might be expected for such a (p,He^2) model for the (p,2p) reaction. It should be noted that such a process is describable in principle by the model of Lim and McCarthy.[14]

Secondly we looked for effects of a final state interaction beyond that contained in the model of Lim and McCarthy. This arrangement kept the mean angle of the two counters, θ_o, constant at 40°, and varied the separation angle between the counters, $\Delta\theta$, from 20° to 40°. This holds the momentum transfer to the recoiling B^{11} constant at about 220 MeV/c, while the relative momentum of the two outgoing protons varies from 60 to 120 MeV/c. The resulting cross section, shown in Fig. 7(b), stays quite constant, showing no significant dependence on the relative momentum of the protons. Thus if any contribution to the forward rise of the cross sections in Figs. 3 or 6 were due to an additional final state interaction, we should have seen a similar rise for this geometry at small $\Delta\theta$. We should point out the smallest $\Delta\theta$ measured here, 20°, was less than the separation angle between the counter for the most forward angles in the symmetric geometry, but was not small enough to provide a general test of a final state interaction effect.

V. EXCITED STATES

The good energy resolution permitted us to separate and identify the first four excited states of B^{11} in the summed energy spectrum (see Fig. 2).

Comparison of $C^{12}(p,2p)B^{11}$ spectra and angular distributions to those of $C^{12}(p,d)C^{11}$, $C^{12}(d,t)C^{11}$, $C^{12}(d,He^3)B^{11}$, which we have studied at the same energy, and inelastic scattering results on B^{11} permit a quite unambiguous assignment of the fifth peak to the 6.76 MeV $7/2^-$ level of B^{11}, with negligible contribution from the positive parity level at 6.81 MeV.

In the shell model interpretation and quasi-elastic scattering approximation, low lying excited states are formed by knocking a proton out of the ground state of C^{12} from a configuration other than pure $(1p_{3/2})^4$. Calculations by Cohen and Kurath[15] using intermediate coupling wave functions, and by Amit and Katz[16], show that C^{12} has a strong admixture of the $(1p_{3/2})^2(1p_{1/2})^2$ configuration. McFarlane[17] has given the following spectroscopic factors for knock-out reactions on C^{12} at 150 MeV: 0.08 for the 2.14 MeV $1/2^-$ state, and 0.13 for the 5.04 MeV $3/2^-$ state, where the ground state factor is unity. This gives the right order of magnitude for the cross sections leading to those states, but fails to give any information about transitions to the 4.46 MeV $5/2^-$ state or the 6.76 MeV $7/2^-$ state. Calculations by Goswami and Pal[18] show an appreciable admixture of 2 particle-2 hole pairs of all orders up to $(2d_{3/2})$. The $(1f_{7/2})$ and $(1f_{5/2})$ admixtures are 1.3% and 0.12% respectively, compared to 10% for $(1p_{1/2})$. These admixtures are quite insufficient to explain the large relative cross sections to the high spin states.

An alternative and inviting explanation would be to consider a two stage process involving the excitation of the C^{12} core to its 2+ state at 4.43 MeV. This state is known to have a strong collective character and to

have a large cross section for excitation by inelastic scattering[19]. The four excited states under consideration then would have a strong admixture of the configuration of a $p_{3/2}$ hole coupled to the 2+ core state of C^{12}. To explain similar results at higher energies, Clegg[20], using the unified model, has calculated expansions of the B^{11} states in terms of the C^{12} 0+ ground state, 2+ state at 4.43 MeV, and 4+ state of the same rotational band at 14.08 MeV. The first four excited states all have a large coefficient of fractional parentage (CFP) to the C^{12} 2+ state. Only the $1/2^-$ state , and to lesser extent the $3/2^-$ state, have appreciable CFP's to the 0+ ground state.

The angular correlations of events leading to these excited states for the symmetrical arrangement are shown in Fig. 8. The $1/2^-$ state has a large forward peak and a deep minimum at about 30°, very similar to the ground state correlation. The $5/2^-$ and $7/2^-$ correlations have quite different patterns, with reduced cross sections at small values of θ; the $3/2^-$ correlation is intermediate between the two extreme patterns. These results are in qualitative agreement with the previous ideas, where the forward angle correlations are largely determined by the one-stage process, and the two-stage process dominates at larger angles. Further evidence[21] for the plausibility of the two-stage excitation process is found in the decay of the low-lying excited states of B^9, which implies a very small 1f -state admixture in B^9.

VI. DISCUSSION

We have shown that the (p,2p) reaction can be studied in the 50 MeV region with sufficient precision to yield useful reaction mechanism information

and to provide new results of spectroscopic interest.

The theoretical fits to our results, in an energy region where distortion and off-energy effects are expected to be severe, are fairly good and at the very least add confidence to the interpretation of data using the same model at higher, more favorable energies. The fits to our data do, however, require changes of the parameters of the distorting potentials from those required to describe elastic scattering. Further investigation is needed to understand this. It should be noted that the theoretical curves of Figs. 3 and 6 represent absolute numbers. No arbitrary normalization is used.

A feature of the experimental results is the comparatively large production of the $7/2^-$ and $5/2^-$ states of B^{11}. Present theoretical descriptions of C^{12} do not seem to provide sufficient quantities of lf-state particles for these to be produced by clean knockout. On the other hand, if their description in terms of a two stage process involving core excitation is correct, a more complicated description than presently available may be necessary even for the ground-state transition.

The nucleus we have studied, C^{12}, is not by any means a typical one. The p-p scattering is further off the energy-shell than it would be for the loosely bound protons in most nuclei, and furthermore strong collective effects are observed in inelastic scattering experiments on this nucleus. Thus, some of the difficulties in interpretation we have encountered may be unusual. We feel that extension of measurements of this type to other nuclei and with energies between 50 MeV and the quasi-elastic region will prove to be of positive value.

REFERENCES AND FOOTNOTES

*Supported by the AEC and the Air Force Office of Scientific Research.

†Now at the University of Maryland, College Park, Maryland.

**NATO Fellow on leave from CNRS, Institute Fourier, Grenoble, France.

‡Permanent address: NASA Lewis Research Center, Cleveland, Ohio.

1. For recent reviews of (p,2p) work see M. Riou, Rev. Mod. Phys. 37, 375 (1965); I. E. McCarthy, ibid. 37, 388 (1965).
2. G. Jacob and Th. A. J. Maris, Rev. Mod. Phys. 38, 121 (1960).
3. K. Dietrich, Phys. Letters 2, 139 (1962); V. V. Balashov and A. N. Boyarkina, Nucl. Phys. 38, 629 (1962); V. V. Balashov, A. N. Boyarkina, and I. Rotter, Nucl. Phys. 59, 417 (1965).
4. H. G. Pugh, D. L. Hendrie, Marc Chabre, and E. Boschitz, Phys. Rev. letters 14, 434 (1965).
5. Th. A. J. Maris, P. Hillman, and H. Tyren, Nucl. Phys. 7, 1 (1958).
6. K. L. Lim and I. E. McCarthy, Phys. Rev. Letters 13, 446 (1964); K. L. Lim and I. E. McCarthy (to be published).
7. R. W. Detenbeck, Nucl. Phys. 74, 184 (1965).
8. H. Tyren, S. Kullander, O. Sundberg, R. Rama Chandrian, P. Isacsson, and T. Berggren, Nucl. Phys. 79, 321 (1966).
9. D. F. Jackson and T. Berggren, Nucl. Phys. 62, 353 (1965).
10. For example, I. E. McCarthy, Rev. Mod. Phys. 37, 388 (1965).
11. F. S. Goulding, D. A. Landis, J. Cerny, and R. H. Pehl, Nucl. Instr. and Methods 31, 1 (1964).
12. R. M. Craig, J. C. Dore, J. Lowe, and D. L. Watson (unpublished).

13. D. C. Peaslee, Phys. Rev. 124, 839 (1961).

14. K. L. Lim and I. E. McCarthy, Phys. Rev. 133, B1006 (1964).

15. S. Cohen and D. Kurath, Nucl. Phys. 73, 1 (1966), and D. Kurath (private communication).

16. D. Amit and A. Katz, Nucl. Phys. 58, 388 (1964).

17. M. H. McFarlane, Nuclear Spectroscopy with Direct Reactions, II. Proceedings, ANL-6878 (1964).

18. A. Goswami and M. K. Pal, Nucl. Phys. 44, 294 (1963).

19. R. W. Peelle, Phys. Rev. 105, 1311 (1957); T. Stovall and N. M. Hintz, Phys. Rev. 135, B330 (1964).

20. S. M. Austin, G. L. Salmon, A. B. Clegg, K. J. Foley, and D. Newton, Proc. Phys. Soc. 80, 383 (1962).

21. D. H. Wilkenson, J. T. Sample, and D. E. Allburger, Phys. Rev. 146, 662 (1966).

FIGURE CAPTIONS

Fig. 1. A simplified block diagram of the experimental arrangement used for the symmetric counter work. The subtractor was not used for the asymmetric work.

Fig. 2. A sample summed energy spectrum $(E_1 + E_2)$ for $C^{12}(p,2p)B^{11}$ at 50 MeV. The positions of the low lying states of B^{11} are indicated.

Fig. 3. The ground state angular correlation resulting from the symmetric $C^{12}(p,2p)B^{11}$ arrangement (see inset), averaged over the range $|E_1 - E_2| \leq 5$ MeV. The dashed line is an estimate of the correlation for $E_1 = E_2$. The solid line is the best fit to the $C^{12}(p,2p)$ work as described in the text.

Fig. 4. $E_1 - E_2$ spectra obtained during the symmetric geometry work. The dashed lines indicate the region over which the averages were taken to obtain the correlation in Fig. 3.

Fig. 5. The differential cross section obtained for the elastic scattering of 17-MeV protons from B^{11}. The solid line is the best fit obtained to the scattering data giving the 4 parameter potential of column 2 of Table I. The dashed line is the prediction obtained from the parameters giving the best fit to the $C^{12}(p,2p)B^{11}$ data; the parameters are listed in column 3 of Table I.

Fig. 6. The angular correlation obtained from the $C^{12}(p,2p)B^{11}$ experiment with one counter held fixed (see inset). The solid line represents the theory using set 3 of the final state optical model parameters. The correlation was averaged over an $E_1 - E_2$ range of ± 5 MeV.

Fig. 7. Angular correlations obtained for the geometries shown in the insets, average over $|E_1 - E_2| < 5$ MeV. The arrangement of Fig. 7(a) maintains the relative momentum of the two outgoing protons at a roughly constant value; that of Fig. 7(b) maintains the momentum transfer to the recoiling nucleus at a roughly constant value.

Fig. 8. The angular correlations obtained for the low-lying excited states of B^{11} from the symmetric $C^{12}(p,2p)B^{11}$ arrangement. The $1/2^-$ and $7/2^-$ level results were averaged over $|E_1 - E_2| < 5$ MeV. The results for the $3/2^-$ and $5/2^-$ levels were averaged over all phase space available in the experiment: $|E_1 - E_2| \lesssim 27$ MeV.

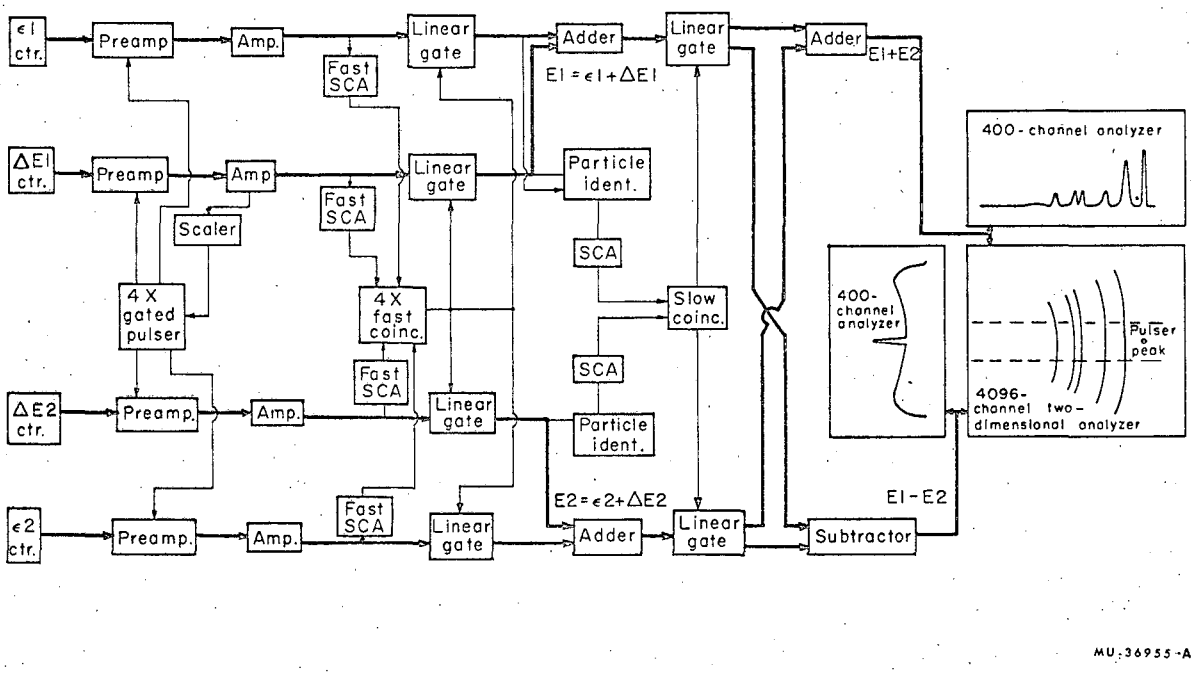

MU-36955-A

Fig. 1

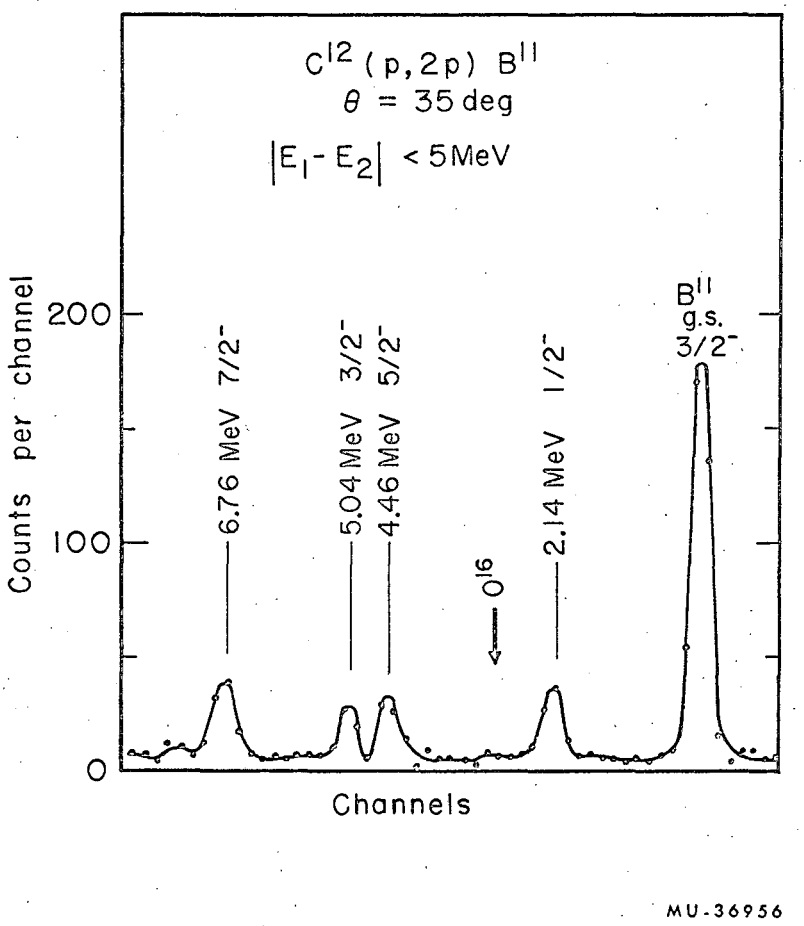
C12 (p, 2p) B11
θ = 35 deg
|E1 - E2| < 5MeV
Counts per channel
200
100
0
6.76 MeV 7/2-
5.04 MeV 3/2-
4.46 MeV 5/2-
O16
2.14 MeV 1/2-
B11 g.s. 3/2-
Channels
MU-36956

Fig. 2

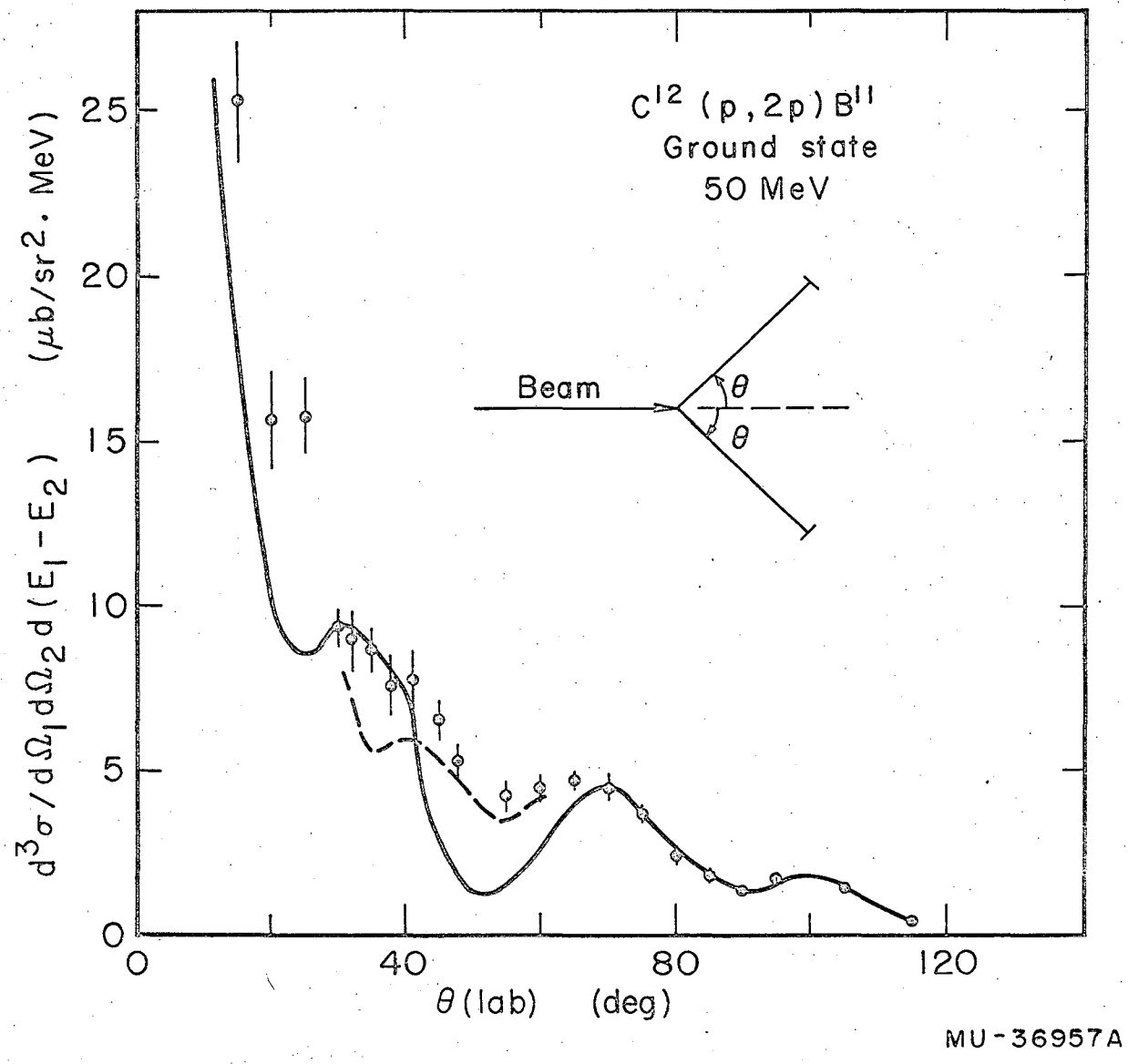
C^{12} (p, 2p) B^{11}
Ground state
50 MeV
Beam
θ
θ
$d^3\sigma/d\Omega_1 d\Omega_2 d(E_1 - E_2)$ (μb/sr². MeV)
0
5
10
15
20
25
0
40
80
120
θ (lab) (deg)
MU-36957A

Fig. 3

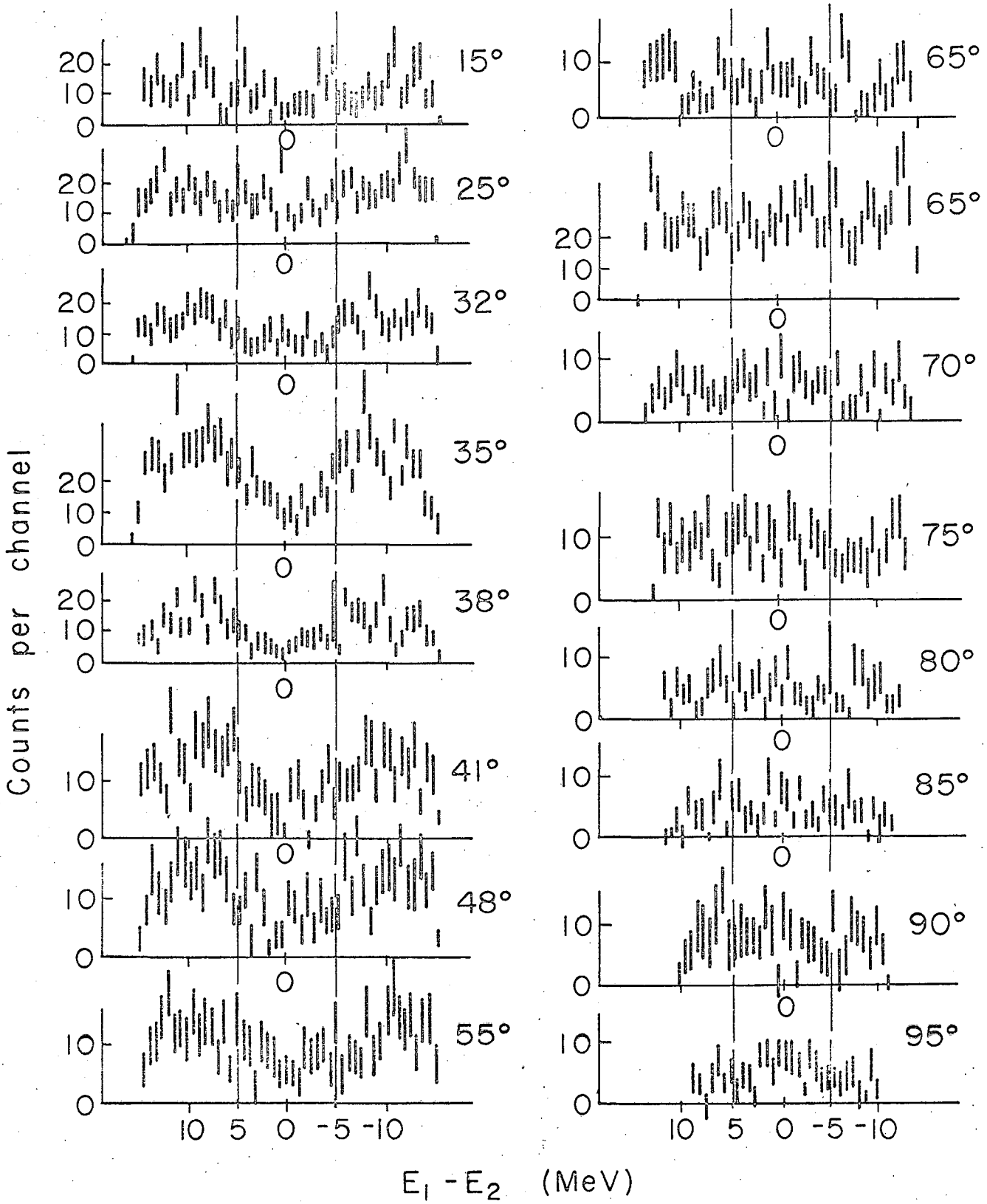

Fig. 4

MU-36958

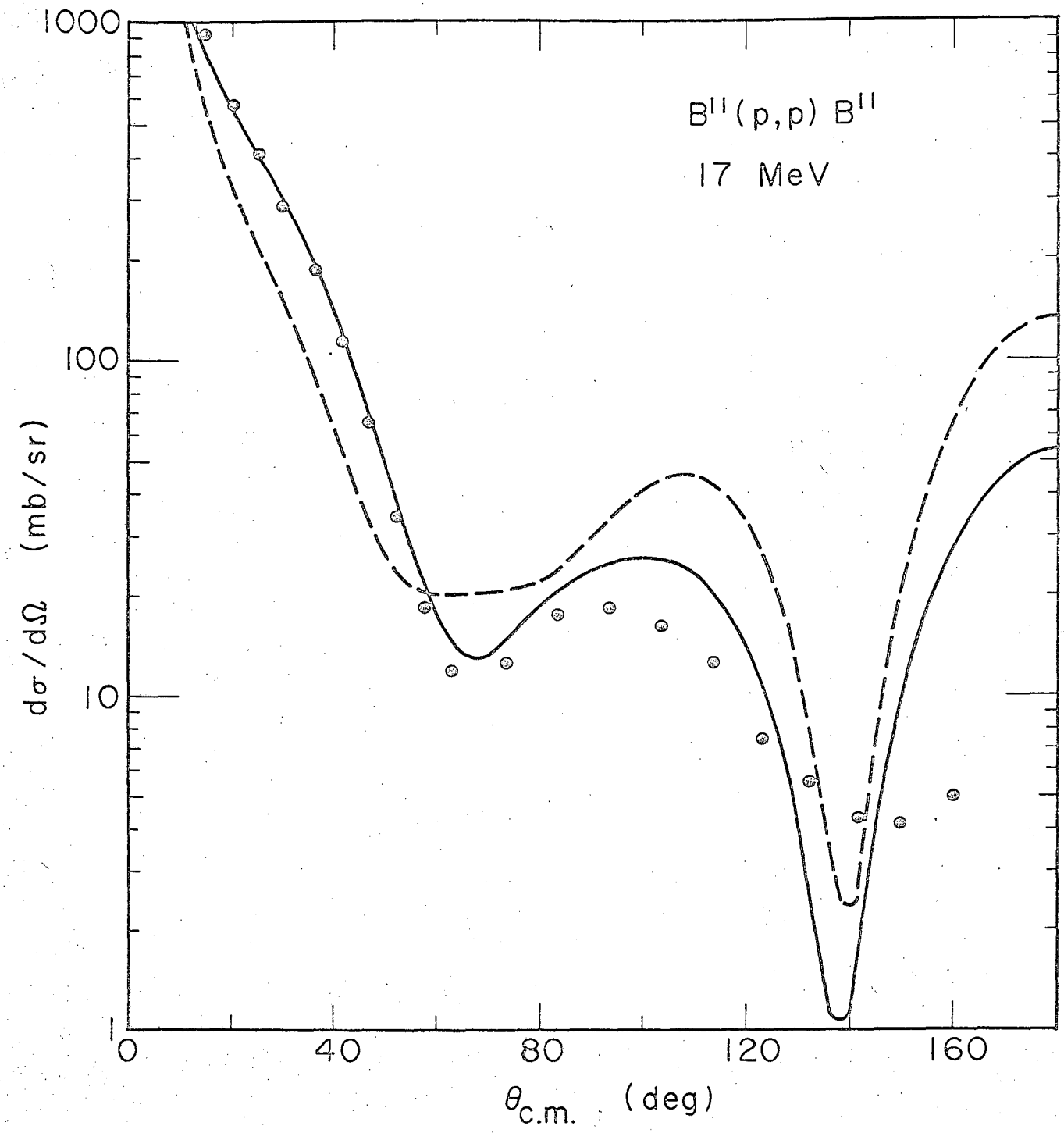

Fig. 5

MU-36959

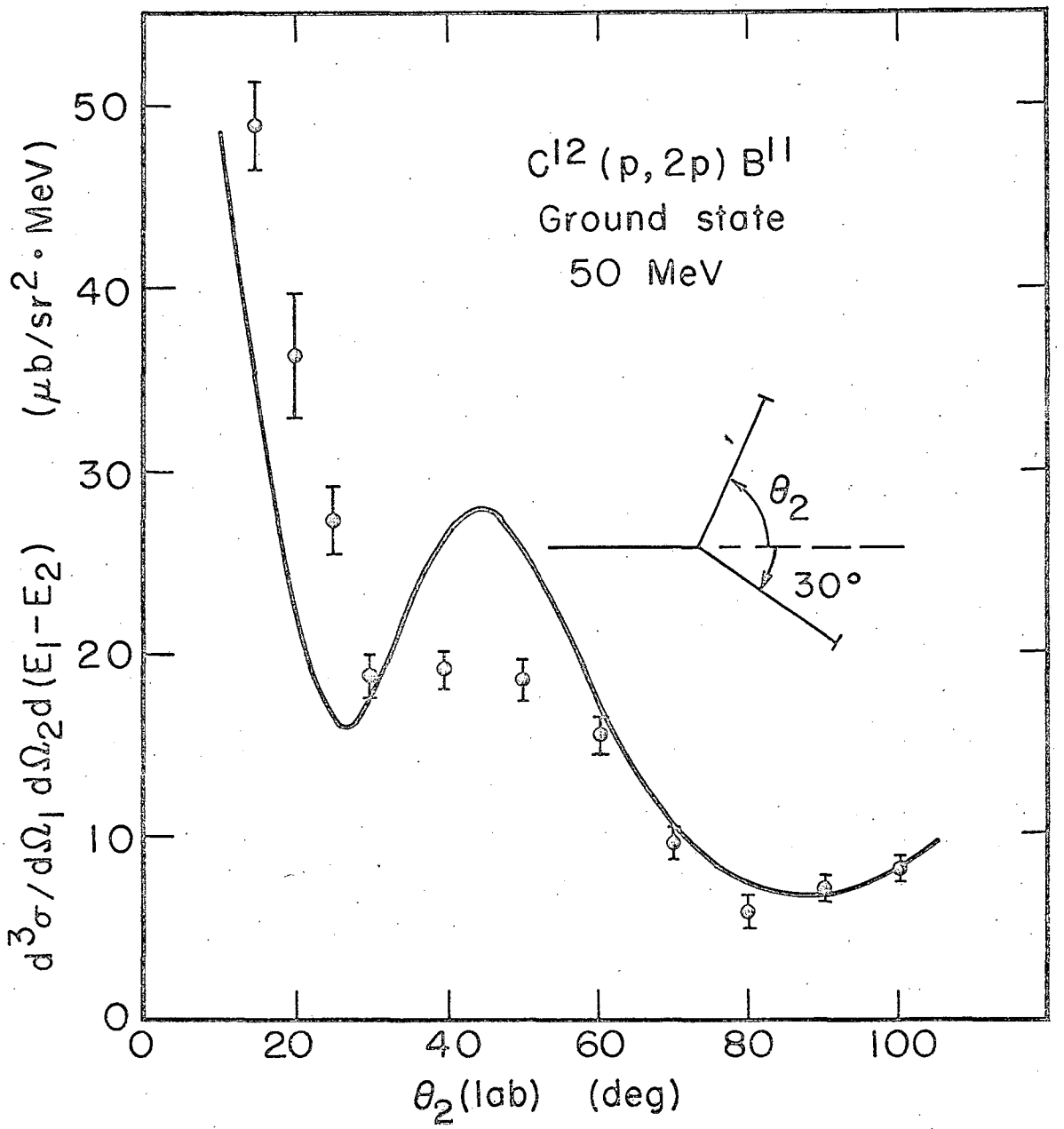

Fig. 6

MU-36960 A

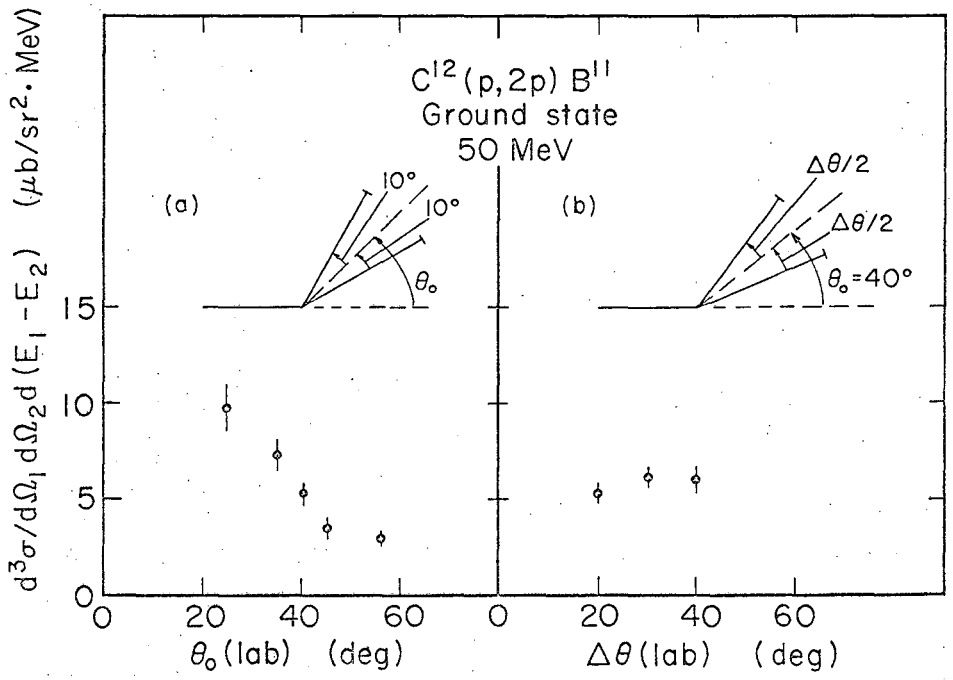
C12(p,2p) B11
Ground state
50 MeV
(a)
10°
10°
θo
(b)
Δθ/2
Δθ/2
θo=40°
d3σ/dΩ1 dΩ2 d(E1-E2) (μb/sr2· MeV)
0
5
10
15
0
20
40
60
θo(lab) (deg)
0
20
40
60
Δθ(lab) (deg)

Fig. 7

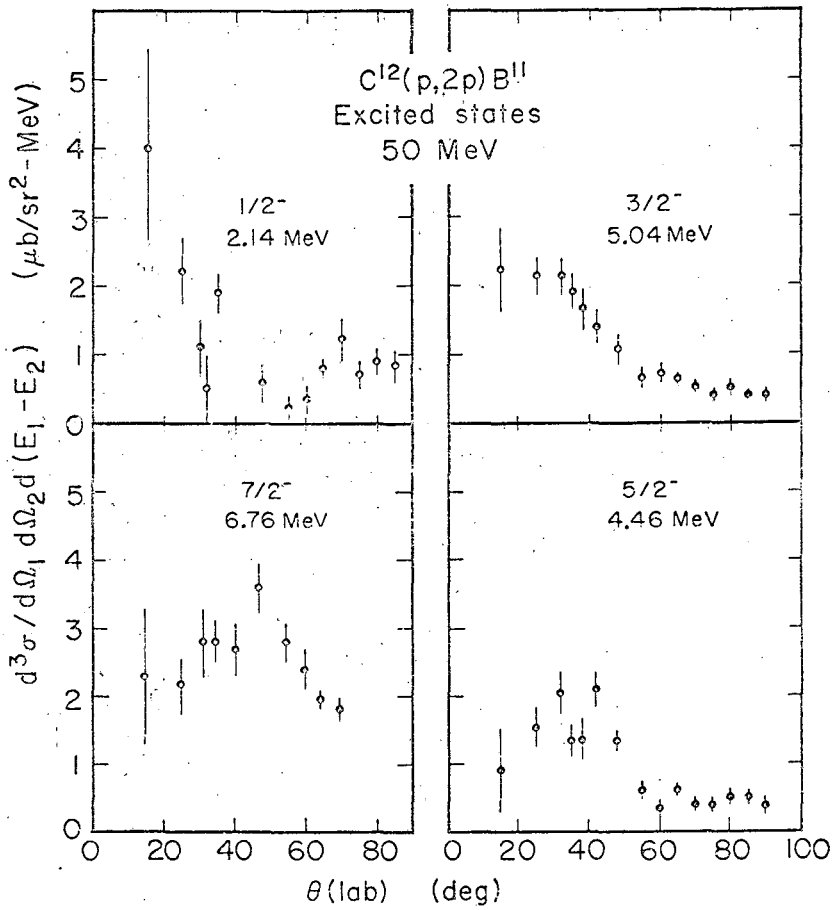
C12(p,2p)B11
Excited states
50 MeV
1/2-
2.14 MeV
3/2-
5.04 MeV
7/2-
6.76 MeV
5/2-
4.46 MeV
d3σ/dΩ1 dΩ2d(E1-E2) (μb/sr2-MeV)
θ(lab) (deg)
0 20 40 60 80
0 20 40 60 80 100
0 1 2 3 4 5
MU-36962

Fig. 8